Impact of Upstream Urbanization on the Urban Heat Island Effects along the Washington–Baltimore Corridor

DA-LIN ZHANG

Department of Atmospheric and Oceanic Science, University of Maryland, College Park, College Park, Maryland

YI-XUAN SHOU

Department of Atmospheric and Oceanic Science, University of Maryland, College Park, College Park, Maryland, and National Satellite Meteorological Center, China Meteorological Administration, Beijing, China

RUSSELL R. DICKERSON

Department of Atmospheric and Oceanic Science, University of Maryland, College Park, College Park, Maryland

FEI CHEN

National Center for Atmospheric Research, Boulder, Colorado*

(Manuscript received 3 November 2010, in final form 12 May 2011)

ABSTRACT

Although there has been considerable research on urban heat island (UHI) effects, most of the previous studies have attributed UHI effects to localized, surface processes. In this study, the impact of upstream urbanization on enhanced UHI effects is examined using surface observations and numerical simulations of an extreme UHI event that occurred on 9 July 2007 over Baltimore, Maryland. Under southwesterly wind, Baltimore experienced higher peak surface temperatures and higher pollution concentrations than did the larger urban area of Washington, D.C. Results from a coupled ultrahigh-resolution mesoscale–urban canopy model with 2001 National Land Cover Data show an advective contribution from upstream urbanization to the UHI event. This dynamical process is demonstrated by replacing Baltimore or its upstream urban areas by natural vegetation (in the model), indicating that the UHI effects could be reduced by as much as 25%. An analysis of the urban–bay interaction reveals the importance of horizontal wind direction in determining the intensity of bay breezes and the urban boundary layer structures. In addition, the vertical growth and structures of UHI effects are shown as layered ''hot plumes'' in the mixed layer with pronounced rising motions, and these plumes can be advected many kilometers downstream. These findings suggest that judicious land use and urban planning, especially in rapidly developing countries, could help to alleviate UHI consequences, including heat stress and smog. They also have important implications for improving the prediction of urban weather, including the initiation of moist convection, air quality, and other environment-related problems.

1. Introduction

By transforming the natural landscape into impervious surfaces, urbanization tends to increase absorption of solar radiation, decrease evapotranspiration, increase runoff, augment surface friction, and release anthropogenic heat, thereby modifying regional near-surface air temperature, horizontal winds, air quality, precipitation, and low-level divergence patterns (e.g., Oke 1987; Bornstein and Lin 2000; Arnfield 2003). Kalnay and Cai (2003) showed that the urban heat island (UHI) effect could influence regional climate. These UHI effects are often responsible for heat stress in the summer (Kunkel et al. 1996).

UHI effects can exacerbate the air pollution. Weaver et al. (2009) summarized model results indicating that

* The National Center for Atmospheric Research is sponsored by the National Science Foundation.

Corresponding author address: Dr. Da-Lin Zhang, Dept. of Atmospheric and Oceanic Science, University of Maryland, College Park, College Park, MD 20742-2425.
E-mail: dalin@atmos.umd.edu

DOI: 10.1175/JAMC-D-10-05008.1

increasing temperatures will increase U.S. ozone air pollution [see also Banta et al. (1998), Cheng and Byun (2008), and Jacob and Winner (2009)]. Observations over the past 20 years show that such a climate change penalty is already observable over the eastern United States (Bloomer et al. 2009, 2010). Zhang et al. (2009) demonstrated that upstream urbanization can have an adverse impact on weather and air quality over cities downstream. They showed that for the Baltimore, Maryland, region, fine particulate matter (the mass concentration of fine particles with diameter less than 2.5 μm, called PM2.5) is positively correlated with surface temperature, especially in summer. In an analysis of surface aerosol concentrations and meteorological conditions over the contiguous United States (Tai et al. 2010), temperature and stagnant winds were found to correlate positively with pollution levels.

Previous studies have revealed that UHI intensity increases with increasing city size, building and population density, contrast between urban surface characteristics and outlying surface conditions, larger-scale flows (e.g., wind speed and direction), cloud cover, topography, and human activity (Oke 1973; Landsberg 1981; Atkinson 2003; Bernstein et al. 2007). Angevine et al. (2003) showed that urban Nashville, Tennessee, has a deeper planetary boundary layer (PBL) with more clouds with higher bases than over surrounding regions; they further showed that this mixed-layer dome extends downwind. Imhoff et al. (2010) used three years of the Moderate (1 km) Resolution Imaging Spectroradiometer (MODIS) skin temperature data to study the UHI effect and its dependence on urban spatial extent and ecological setting. They showed that the mid-Atlantic region with natural vegetation of broadleaf deciduous forest has relatively strong UHI effects. They found that urban-minus-rural temperature differences scale in general with the logarithm of the developed area, but not all cities follow this trend.

Although much of our knowledge of the UHI effects can be attributed to the analyses of numerous field observations (e.g., Allwine et al. 2002; Rotach et al. 2005), mesoscale models have been used as an important research tool to advance our understanding of the physical processes associated with the UHI effects and their interaction with ambient differential land cover (DLC)–induced circulations as well as the structures and evolution of the urban PBL. Earlier modeling studies have treated urban surfaces as one land-use type and neglected the geometrical effects of an urban canopy (e.g., Rozoff et al. 2003; Grossman-Clarke et al. 2005). Sophisticated urban canopy models, including the urban building geometry and the distribution of major roads and industry as well as anthropogenic heat release, have recently been developed to study UHI effects, the urban PBL, and various urban environment–related problems (Kusaka et al. 2001; Martilli et al. 2002; Holt and Pullen 2007; Miao and Chen 2008; Miao et al. 2009). In particular, the rapid growth of computing power and the availability of the U.S. multiagency 2001 30-m-grid-spacing National Land Cover Data (NLCD 2001; for more information see online at http://www.mrlc.gov/about.php) have allowed us to perform extra-high-resolution simulations of UHI for North American cities with realistic specification of the underlying surface characteristics (Zhang et al. 2009).

The UHI effects are pronounced on most sunny summer days over the Washington–Baltimore corridor (WBC) with extremely high ozone concentrations exceeding the 1-h National Ambient Air Quality Standard (NAAQS) during the past decades (Vukovich and Sherwell 2003). Previous studies indicate that the WBC's UHI intensity has increased since the early 1950s as a result of rapid growth in population and changes in land use (Landsberg 1979; Viterito 1989; Brazel et al. 2000). Indeed, the two metropolitan areas have been nearly merged with the expansion of the city of Columbia, Maryland, and small towns between during the past few decades. In addition, Ntelekos et al. (2007) find that rapid urbanization in the Baltimore metropolitan area may account for increased thunderstorm frequency as the enhanced UHI circulations interact with the Chesapeake Bay breezes and alter the hydrological response to heavy rainfall. Of particular relevance to the study presented here is that, under certain weather conditions, higher surface temperatures and ozone concentrations were observed in Baltimore than in Washington, D.C. (Zhang et al. 2009). These differences could not be attributed to either urban size or urban population, since both are relatively smaller in the Baltimore than in the Washington metropolitan area (as reported online at http://en.wikipedia.org/wiki/Baltimore%E2%80%93Washington_Metropolitan_Area).

Although the UHI effects for isolated cities are well documented in the literature (e.g., Bornstein 1968; Oke 1987, 1995; Arnfield 2003), few studies have examined the interaction of urban circulations between neighboring metropolitan regions, especially the influences of upstream urbanization on the UHI effects. One exception is the study of Ohashi and Kida (2004) who examine the transport of moisture and air pollutants between two neighboring cities in Japan using a simplified geometric model with idealized landscapes and calm larger-scale flows. Their results with the calm large-scale flow cannot be applied to the above-mentioned scenarios along the WBC.

The rapid urbanization and regional climate changes occurring worldwide in recent decades motivate us to examine the hypothesis that UHI effects can propagate well downwind of a given urban area. Zhang et al. (2009) used high-resolution simulations to investigate the extreme episode of 9 July 2007, when Baltimore experienced a peak (2 m) surface temperature T_{SFC} of 37.5°C and an 8-h mean ozone concentration of 131 ppbv or an air quality index of 187 that was in the unhealthy NAAQS (as reported online at http://alg.umbc.edu/usaq/archives/2007_07.html) category. Although the urban area of Washington, D.C. is larger than that of Baltimore, Maryland, Baltimore was hotter—the T_{SFC} was about 1.5°C higher than that observed in Washington. Zhang et al. (2009) showed that at least part of this difference can be attributed to upstream urbanization.

This study will delve more deeply into the effects of upstream urbanization with the objectives of examining 1) the spatial and diurnal variation of the UHI effects, 2) the diurnal variation of horizontal winds in the urban PBL, 3) the different PBL structures between urban and nearby rural regions, and 4) the interactions between the UHI circulations and bay breezes. Section 2 describes a coupled mesoscale weather prediction model with an urban canopy model, the model configuration, and the urban–rural land-use characteristics over the WBC. Section 3 presents a numerical case study of the 8–9 July 2007 UHI events, including the large-scale flow conditions, and model verifications. Section 4 shows validation of the above-mentioned hypothesis by examining the impact of upstream urbanization through diagnostic analysis of the model simulation and two sensitivity tests. Section 5 examines the normal-flow circulations and different PBL structures between the urban and rural areas, and their interaction with the Chesapeake Bay breezes, along the WBC. A summary and concluding remarks are given in the final section.

2. Model description

The numerical model used for this study is a two-way interactive, quadruply nested version of the Weather Research and Forecast (WRF-V2.2) model (see Skamarock et al. 2005), coupled with a single-layer urban canopy model (UCM) (see Kusaka et al. 2001; Chen et al. 2004, 2010). The quadruply nested domains have x, y dimensions of 181×151, 244×196, 280×247, and 349×349 with grid sizes of 13.5, 4.5, 1.5, and 0.5 km, respectively. The outermost domain covers the eastern half of the United States and a portion of Canada and the Atlantic Ocean, whereas the innermost domain provides enough coverage for the generation and evolution of the UHI effects and nearby DLC-induced circulations over the WBC (Fig. 1). All domains use 31 σ levels[1] in the vertical direction with 20 layers in the lowest 2 km to better resolve the evolution of the PBL. The model top is defined at 50 hPa.

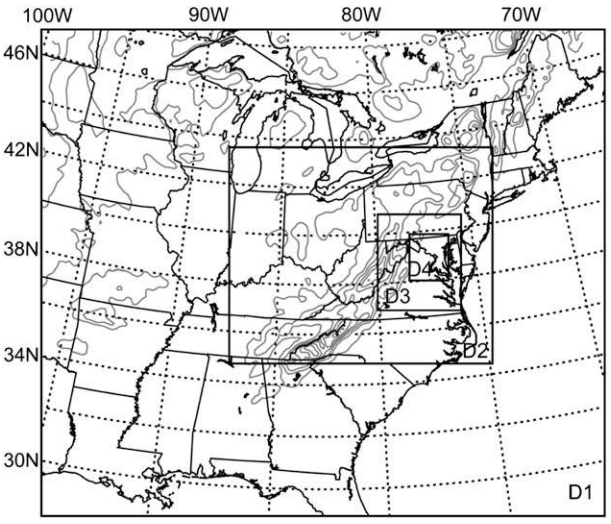

FIG. 1. Model meshes with horizontal resolutions of 13.5, 4.5, 1.5, and 0.5 km for domains D1, D2, D3, and D4, respectively; terrain heights (m) are contoured at 200-m intervals starting from 250 m.

The WRF model physics used include 1) a three-class microphysical parameterization (Hong et al. 2004), 2) the Mellor–Yamada–Janjić planetary PBL scheme (Mellor and Yamada 1974; Janjić 1994), 3) the "Noah" land surface scheme in which four soil layers and one canopy with the U.S. Geological Survey (USGS) 24-category land uses are incorporated (Chen and Dudhia 2001), 4) the Grell and Devenyi (2002) ensemble cumulus scheme as an additional procedure to treat convective instability for the first two coarsest-resolution domains, and 5) the Rapid Radiative Transfer Model for longwave radiation with six molecular species (Mlawer et al. 1997) and the Goddard shortwave radiation scheme (Chou and Suarez 1994).

The single-layer UCM is used with three-category urban surfaces at 30-m grid spacing, that is, low-intensity residential (Fig. 2b), high-intensity residential (Fig. 2c), and commercial/industrial/transportation coverage (Fig. 2d) on the basis of the NLCD 2001 data. The coupled Noah model–UCM takes into account the dynamical and thermodynamical properties of roofs, walls, and roads as well as some anthropogenic effects. One can see clearly from Fig. 2 the distribution of high-intensity residential and commercial/industrial areas (in terms of

[1] The 31 σ levels are given as follows: 1.0, 0.9969, 0.9935, 0.9899, 0.9861, 0.9821, 0.9777, 0.9731, 0.9682, 0.9629, 0.9513, 0.9382, 0.924, 0.9088, 0.8925, 0.8752, 0.8661, 0.8471, 0.8261, 0.8008, 0.7704, 0.7341, 0.6911, 0.6406, 0.5806, 0.506, 0.4161, 0.3119, 0.1982, 0.0804, and 0.

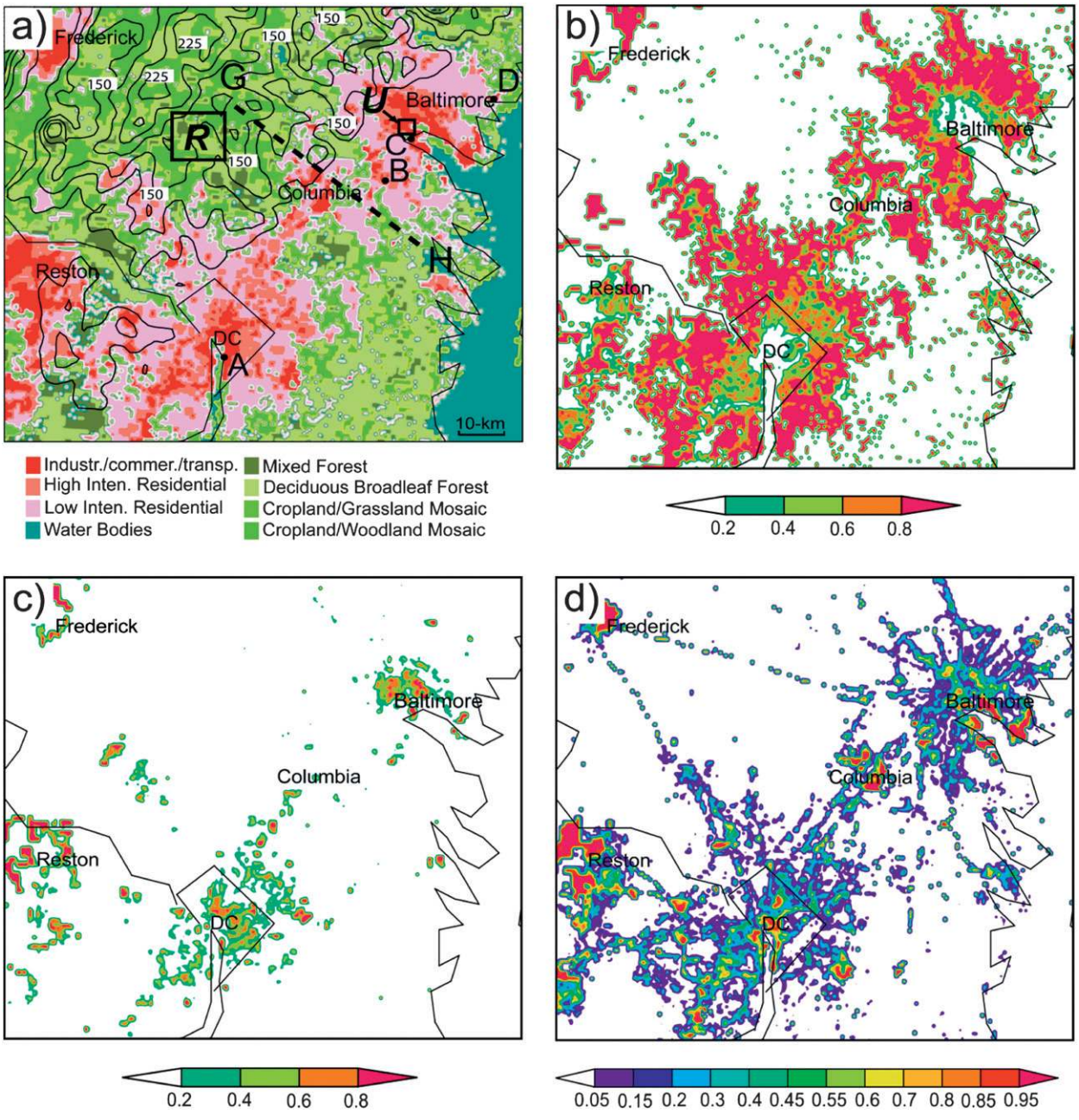

FIG. 2. (a) Dominant land use (shaded) and terrain heights (solid contours, at intervals of 25 m starting from 120 m), (b) low-intensity residential coverage (%), (c) high-intensity residential coverage (%), and (d) commercial/industrial/transportation coverage (%) over an x, y subdomain (115 km × 88 km) of D4. In (a), letters A–D denote the locations of surface stations DCA, BWI, DMH, and APG, respectively, which will be used in Fig. 6; boxes U and R represent the urban and rural area used to estimate the UHI effects in Figs. 7 and 11; and thick dashed line G–H indicates the boundary of land-use changes used in expts NUH and RUR in Fig. 8.

percentage coverage in each grid box) over the central business districts (CBDs) of Baltimore; Washington; Columbia; Reston, Virginia; and Frederick, Maryland (Fig. 2c), and major interstate highways (e.g., I-70 between Frederick and Baltimore, I-270 between Frederick and Washington, I-95 and Maryland Route 295 between Baltimore and Washington) plus the beltways of Baltimore and Washington (Fig. 2d). A panhandle-shaped urban region, dominated by the low-intensity residential category, extends from Washington northwestward (Figs. 2a,b) and will be shown in sections 4 and 5 to play a role in enhancing the UHI effects downstream.

Note 1) that the Washington–Baltimore area underwent substantial urban expansion between 2001 and 2007 (http://en.wikipedia.org/wiki/Baltimore%E2%80%93Washington_Metropolitan_Area) and that this growth will have significant impact on the UHI effects along the WBC, 2) that the foothills of the Appalachians, with the highest peak of less than 250 m above sea level (Figs. 1 and 2a), produce little impact on the UHI effects during the daytime but that their topographical impact at night may not be negligible (see Zhang et al. 2006), and 3) that the presence of Chesapeake Bay and the Potomac River could affect the UHI effects of Baltimore and Washington, respectively, through the DLC-induced circulations. All of these effects will be shown in the next three sections.

The combined land uses of the USGS 24-category land cover and three-category urban data are given in Fig. 2a, which shows the distribution of dominant land use with large DLC between urban and rural areas. In the combined land-use data, the NLCD 2001 is used to determine roughness length, albedo, zero plane displacement height, emissivity, and the other surface parameters (e.g., building height and sky view factor) that influence the surface energy budget over urban areas. In this coupled model, the momentum, heat, and moisture fluxes are computed according to the dominant land-use/land-cover type from the NLCD 2001. If the dominant land-use/land-cover for a given model grid box is one of the three urban classes, the UCM will be called after the Noah land surface scheme handles the fluxes from natural and vegetated urban surfaces. That is, for simplicity, an urban grid box is first treated as a crop or grassland mosaic in Noah. A weighted average of the fluxes from the Noah and UCM schemes will then be performed, depending upon the urban fraction of the grid box under consideration. See Kusaka et al. (2001), Chen et al. (2004, 2010), Holt and Pullen (2007), and Miao et al. (2009) for more details.

The coupled WRF–Noah–UCM system is initialized at 1200 UTC (0700 LST) 7 July 2007 and is integrated for 72 h until 1200 UTC 10 July 2007. The model initial conditions and its outermost lateral boundary conditions are taken from the National Centers for Environmental Prediction (NCEP) 1°-grid-spacing Global Forecast System Final Analyses (GFS-FNL), with the latter updated every 6 h.

3. Model verification and the UHI effects

To help to understand the development of the present UHI events, we show first the large-scale flows from the NCEP GFS-FNL at 1200 UTC 8 and 9 July in Figs. 3a and 3b, respectively. The WBC and its surroundings were dominated by weak westerly winds with weak thermal gradients associated with the Bermuda high, which are typical summertime conditions over the region. A shortwave trough passed by prior to the model initial time, however, bringing some precipitation over the WBC (not shown). Moreover, as a low pressure system, centered in Alabama on 8 July, moved northeastward, a stronger southwesterly flow began to develop to the south of the WBC on the early morning hours of 9 July (cf. Figs. 3a,b) and persisted until 1800 UTC 11 July (not shown). As shown in Fig. 4d, this southwesterly flow reached Baltimore in the early afternoon and increased T_{SFC} there. As will be shown later, the resulting distribution of T_{SFC} contributed to a stronger UHI in Baltimore. Next, we verify the simulated surface features before using the model results to validate our hypothesis.

Figure 4 compares the simulated surface skin temperature T_{SKIN} with the MODIS-measured T_{SKIN} at 1840 UTC 8 July and 1745 UTC 9 July 2007. Sharp contrasts in the measured T_{SKIN} between urban (colored in red), suburban (colored in yellow), and rural (colored in blue) areas are clearly evident; they agree well with the distinct land-use categories (cf. Figs. 4a,c and 2a), since T_{SKIN} represents the footprint of land-use characteristics (Jin et al. 2005). Because the MODIS data on 9 July (at 1245 LST) were available about 1 h earlier, the urban and suburban signals were slightly weaker than those on 8 July (at 1340 LST) (cf. Figs. 4a,c). As will be seen from the observed T_{SFC}, the UHI signals on 9 July appeared to be stronger than those on 8 July. Some minor differences in T_{SKIN} exist, for example, over Columbia and Frederick, but they could be attributed to rapid urbanization that occurred since 2001. It is obvious from the MODIS data that significant UHI effects were present over Washington, Columbia, Baltimore, Reston, and Frederick as well as over many small towns.

The hottest locations with the peak T_{SKIN} of more than 45°C in Baltimore, Reston, and Frederick correspond to the commercial/industrial/transportation and high-intensity residential categories, where the CBDs are located; they were more than 10°C higher than their ambient rural regions at this early afternoon hour. Note the generation of a large hot spot on 8 July (Fig. 4a) but two small hot spots on 9 July (Fig. 4c) in the CBD of Baltimore. In addition to the 1-h difference in receiving the MODIS data, the relatively colder mean T_{SKIN} on 9 July could also be attributed partly to the large errors in retrieving the MODIS measurements in the presence of high aerosol concentrations on such a hot day, having a peak T_{SFC} of 37.5°C, as compared with 8 July, with a peak T_{SFC} of 35.5°C. Wan (2008) and Wan and Li (2008) showed that such errors could be more than 2°C in cases of heavy aerosol loading over urban regions, as

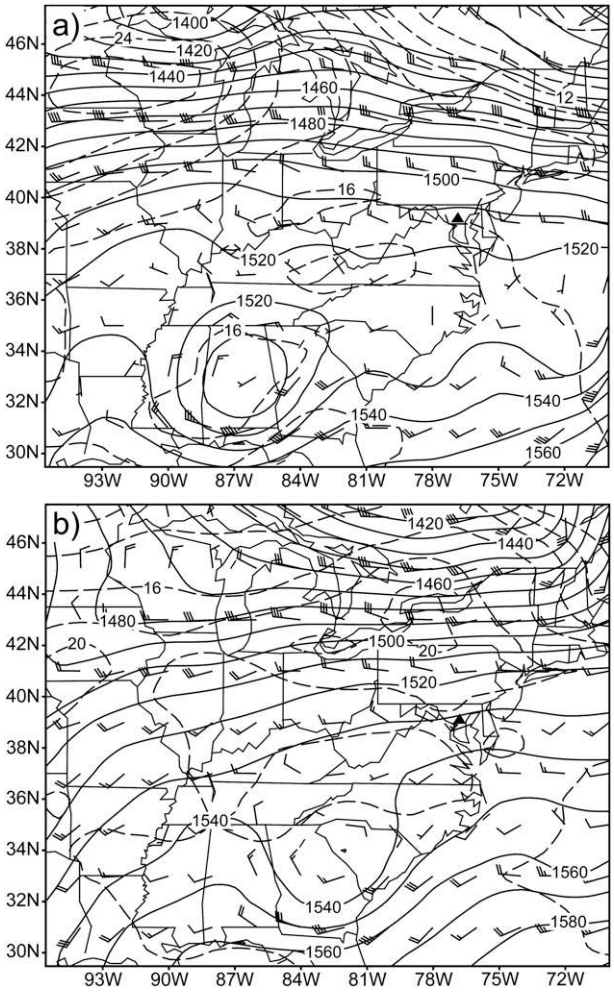

FIG. 3. NCEP's final analysis of geopotential height (solid contours, every 10 m), temperature (dashed contours, every 2°C), and wind barbs (a full barb is 5 m s^{-1}) at 850 hPa at (a) 1200 UTC 8 Jul and (b) 1200 UTC 9 Jul 2007.

ocurred in Baltimore on 9 July (see http://alg.umbc.edu/usaq/archives/2007_07.html). In fact, the mean aerosol optical depth on 9 July was nearly 2 times that on 8 July over the WBC (see online at http://aeronet.gsfc.nasa.gov/).

It is encouraging from Fig. 4 that despite the use of large-scale initial conditions the coupled WRF–Noah–UCM reproduces well the observed UHI effects on both days, and especially the sharp contrasts among urban, suburban, and rural areas. In fact, the simulated UHI patterns resemble those of the land cover better than do the measured data (cf. Figs. 2a and 4b,d), because of the use of year 2001 land-use data. In particular, the model could even capture the UHI effects of in-state highways of I-70 and I-270 as well as the other major highways. In contrast, Maryland Route 295, the Baltimore–Washington Parkway running northeast–southwest between these two cities, has tree cover in the median and off the shoulders—it does not have a discernible heat signature. Some differences still exist; for instance, 1) the UHI effects over some small towns and suburban areas are missed or underestimated because of the use of the outdated land-use data and 2) the coverage of T_{SKIN} between 44° and 46°C over the urban areas is slightly overestimated (cf. Figs. 4c,d).

The model also reproduces reasonably well the observed surface winds (V_{SFC}; colored in white) at several stations, except for wind directional errors at Washington National Airport (DCA) and to its east (see Fig. 2a for the station location) on 8 July. In general, both the observed and simulated V_{SFC} are near westerly on 8 July, and began to shift to southwesterly along the WBC at 1745 UTC 9 July, as also indicated by the larger-scale flows (cf. Figs. 4b,d and 3b). In terms of spatial pattern, the prevailing V_{SFC} along the WBC turn from near southerly on the upwind side of Washington to southwesterly over Columbia and then to near westerly on the northern side of Baltimore (Fig. 4d). As will be seen later, the southwesterly flows dominate the WBC by 2030 UTC 9 July.

Moreover, one can see the distribution of the Chesapeake Bay breeze and its associated convergence zone, part of which has entered the city of Baltimore from its harbor, the urban V_{SFC} that are about 2–4 m s^{-1} weaker than those over rural areas because of the presence of high roughness elements in cities, as well as the upstream-diffluent and the downstream-confluent flow patterns across both Washington and Baltimore. Relatively weaker surface flows over the urban areas are also consistent with the finding of about 25% reduction of V_{SFC} over cities by Landsberg (1981).

The sharp thermal contrasts and pronounced UHI effects shown in Figs. 4a,c could not be simulated without use of the UCM. This is demonstrated in a sensitivity simulation in which the UCM is turned off (experiment NUCM) from the control run (experiment CTL) shown in Fig. 4. Results, given in Fig. 5, show that use of the Noah land surface scheme alone tends to produce weaker and smoother UHI effects than those in CTL. In particular, the observed high T_{SKIN} at the CBDs and pronounced T_{SKIN} along the suburban corridor between Washington and Baltimore are not simulated (cf. Figs. 5 and 4c). Moreover, the urban V_{SFC} experiences little reduction in comparison with that in CTL, causing different flow patterns near the urban–rural interface. All these indicate the importance of using the UCM to capture the timing and locations of the observed UHI effects, provided that the urban land-use information is up to date.

Figure 6 compares the diurnal cycles of T_{SFC} and V_{SFC} between the simulation and observations that are taken

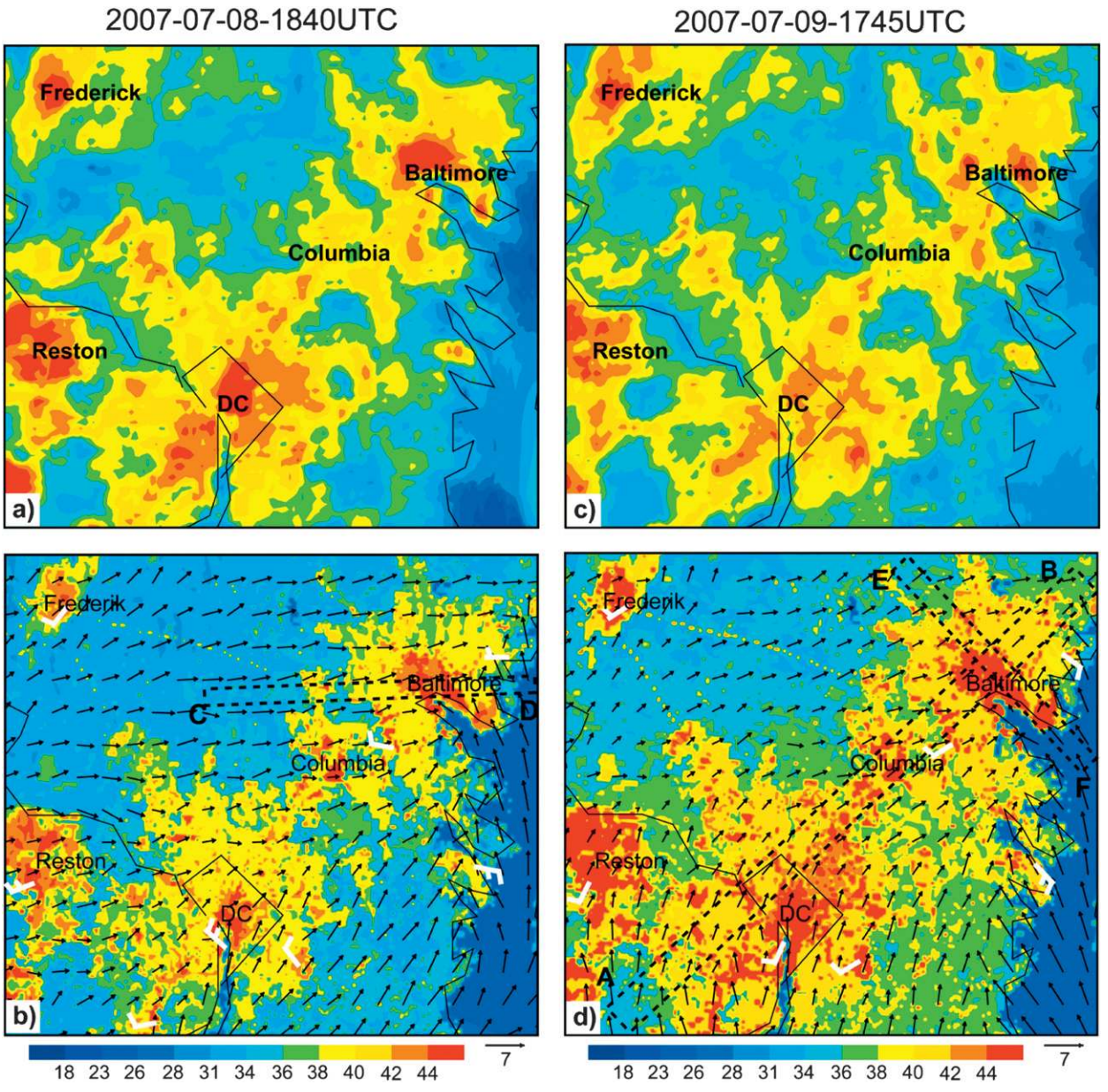

FIG. 4. Comparison of (a) and (c) the MODIS-observed (1-km resolution) T_{SKIN} (°C) with (b) and (d) the simulated T_{SKIN} with surface wind vectors plotted at 6-km grid intervals superimposed over a subdomain of D4, valid at 1840 UTC 8 Jul and 1745 UTC 9 Jul 2007, respectively. Wind barbs (colored in white) in (b) and (d) denote a few available observed surface winds; a full barb is 5 m s^{-1}. Zones A–B in (d), C–D in (b), and E–F in (d), enclosed by dashed lines, denote the locations of the area-averaged vertical cross sections used in Figs. 9, 10, and 12.

at stations DCA (Fig. 6a), Baltimore–Washington International Airport (BWI) (Fig. 6b), Baltimore's Science Center (DMH) (Fig. 6c) near Baltimore's harbor, and Aberdeen Proving Grounds Airport (APG) (Fig. 6d) in Baltimore's northern suburbs (see Fig. 2a for their locations) during the period of 0400 UTC 8 July–0400 UTC 10 July. Note that these surface stations are not ideally suitable for studying the UHI effects because none of them is located in the CBD of Washington, Columbia, or Baltimore. Nevertheless, two important features should be noted. First, the observed peak T_{SFC} on 9 July was higher than that on 8 July at all of the stations (Figs. 6b–d), except at DCA where little difference in the peak T_{SFC} (up to 36°C) occurred during the 2-day period (Fig. 6a). In particular, station DMH shows a peak T_{SFC} of 37.5°C on 9 July, which was about 1.5°C higher than that

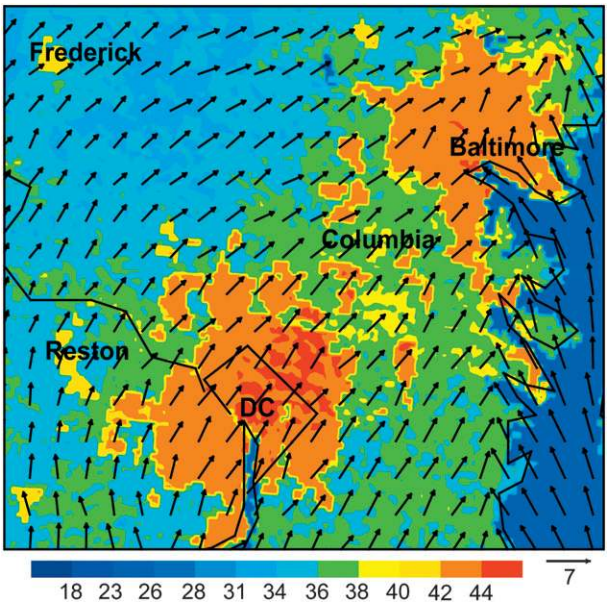

FIG. 5. As in Fig. 4d, but for a sensitivity simulation in which the UCM is turned off (expt NUCM).

on 8 July (Fig. 6c). Second, on 9 July the peak T_{SFC} at DMH (i.e., Baltimore) was about 1.5°C higher than that at DCA. As mentioned before, the high T_{SFC} in Baltimore is hypothesized to result from upstream urbanization along the WBC. This appears to be also true for the high T_{SFC} at DCA on 8 July that is due partly to its large urban coverage and population, as well as its location downstream of Reston.

The coupled model appears to reproduce well the diurnal phase of T_{SFC} during the 2-day period and the peak T_{SFC} on 9 July at DCA, BWI, and APG. It underpredicts the peak T_{SFC} by 1.0°–1.5°C at all four stations on 8 July and by less than 1.0°C at DMH on 9 July, however. That is, the simulated peak T_{SFC} at DMH and DCA on 9 July are 36.5° and 36°C as compared with the observed 37.5° and 36°C, respectively. These errors appear to be closely related to the origin of upstream surface air, which is the hypothesis to be examined herein. For example, the negative T_{SFC} error at DCA on 8 July occurs because the simulated surface air is southwesterly from the upstream rural area whereas the observed air was going through the warm urban region (including Reston) to the west—that is, the wind-directional errors as mentioned before (see Fig. 4b). In a similar way, because of its location at Baltimore's harbor, the T_{SFC} error at DMH on 9 July appears to be caused by too-early intrusion of the simulated bay breezes, as indicated by near-constant T_{SFC} during the period of 1500–1900 LST; this will be further shown in section 5. Nevertheless, we believe that the 1°C negative (positive) bias in T_{SFC} (T_{SKIN}) at DMH is not relevant, since T_{SFC} is a diagnostic variable at a single point in the coupled model; the 1.5°C difference in T_{SFC} between stations DCA and DMH is significant, however. As will be seen in the next section, the T_{SFC} differences over the CBDs of the two cities would make more sense on the UHI effects than those at the single locations. Note that the rural T_{SFC} on 9 July seem to be slightly higher than that on 8 July, likely because of decreasing evaporation of soil moisture after the regional rainfall event on 7 July. Nevertheless, this has little effect on the major rural–urban difference in T_{SFC}.

The model overpredicts systematically the minimum T_{SFC} at the dawn time because of the generation of too-strong downward mixing of high–potential temperature (θ) air by the Mellor–Yamada–Janjić PBL scheme, as discussed by Zhang and Zheng (2004). For the same reason, the model overpredicts V_{SFC} at night (Figs. 6e–g), especially around dawn when the observed V_{SFC} in Baltimore were nearly calm. Since we focus mainly on the daytime UHI effects in this study, the nighttime-related PBL and UHI effects will not be examined herein. In this regard, the coupled WRF–UCM reproduces well the magnitude of the daytime V_{SFC}, with its peak magnitude coinciding roughly with the peak T_{SFC} (cf. Figs. 6a–d and 6e–h). This result is consistent with that of Zhang and Zheng (2004) who find that the diurnal cycles of V_{SFC} are generally in phase with those of T_{SFC}. Nevertheless, the model does not seem to capture the timing of the first impulse in V_{SFC} in the early afternoon, namely, lagging behind the observed by about 2–3 h. This error could be attributed partly to the use of the local K-mixing scheme (though through turbulent kinetic energy), as compared to nonlocal eddy mixing (see Zhang and Zheng 2004; Zhang and Anthes 1982), and partly to some local (nonresolvable) forcing.

Note that the diurnal cycle of V_{SFC} is generally opposite in phase to that in the PBL (V_{PBL}). Namely, weaker (stronger) horizontal winds occur typically in the PBL, as compared with stronger (weaker) V_{SFC}, during the afternoon (early morning) hours (see Zhang and Zheng 2004). This can be seen by qualitatively comparing the diurnal cycles of V_{SFC} and V_{PBL} between Figs. 6 and 7a. The urban V_{PBL} exhibits an inertial oscillation, similar to that shown in Zhang et al. (2006), with the smallest (i.e., 2–3 m s^{-1}) and largest (i.e., 8–9 m s^{-1}) magnitudes occurring during the periods of 1100–1600 and 0100–0600 LST, respectively. The decoupling of the surface layer from the layers above accounts for the large differences between V_{SFC} and V_{PBL} during the nighttime. In contrast, similar magnitudes of V_{SFC} and V_{PBL} during the daytime result from the strong vertical mixing of horizontal momentum in terms of both wind speed and

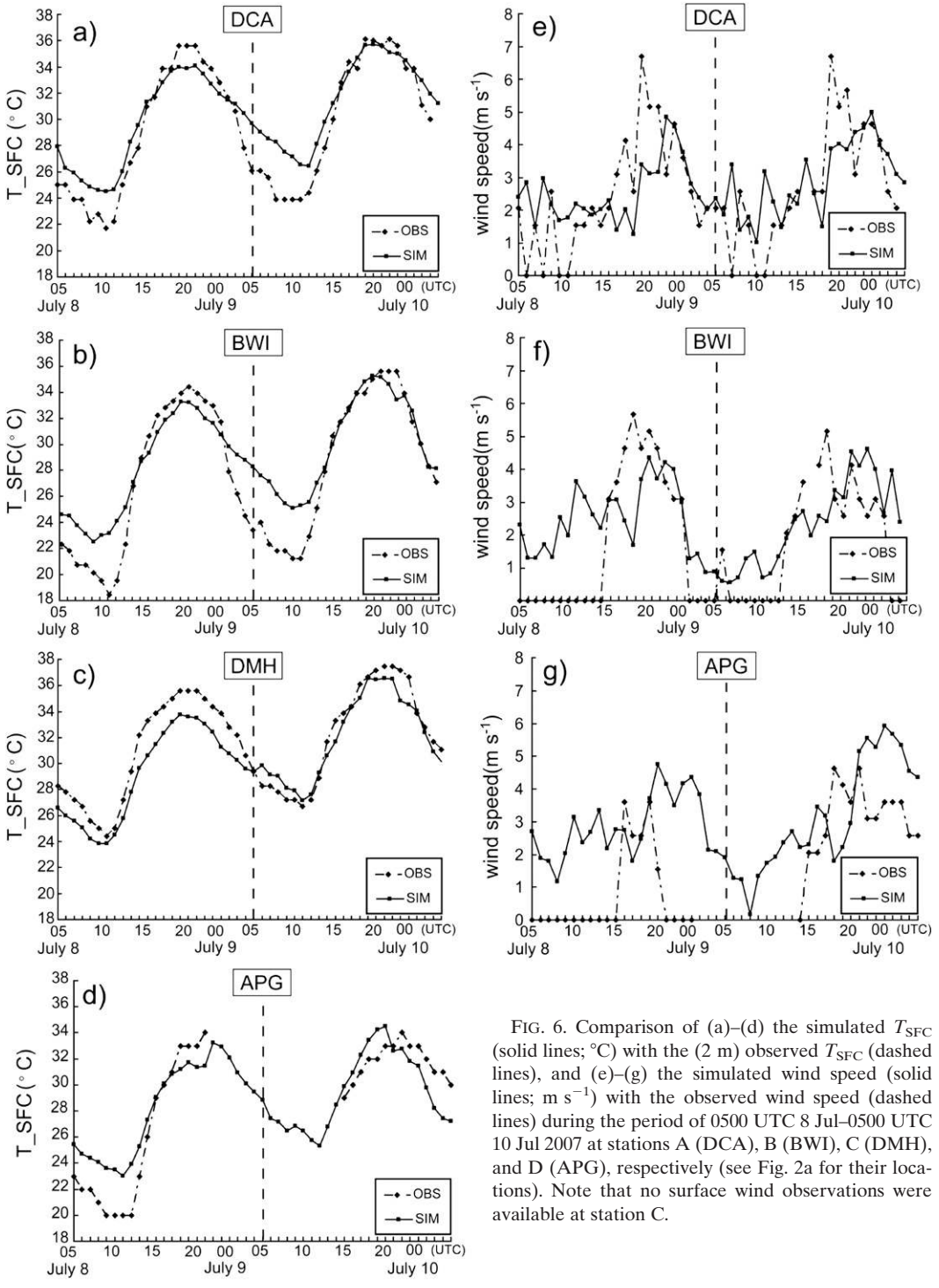

FIG. 6. Comparison of (a)–(d) the simulated T_{SFC} (solid lines; °C) with the (2 m) observed T_{SFC} (dashed lines), and (e)–(g) the simulated wind speed (solid lines; m s^{-1}) with the observed wind speed (dashed lines) during the period of 0500 UTC 8 Jul–0500 UTC 10 Jul 2007 at stations A (DCA), B (BWI), C (DMH), and D (APG), respectively (see Fig. 2a for their locations). Note that no surface wind observations were available at station C.

direction. In particular, Fig. 7a shows that, like V_{SFC}, V_{PBL} also varies from westerly to southwesterly during the afternoon hours.

Figure 7b summarizes the diurnal variations of the UHI effects along the WBC by comparing the simulated time series of the area-averaged T_{SFC} over the CBDs, suburban, and rural areas. The mean T_{SFC} difference between the CBDs and rural area is the largest at midnight (~4.5°C), followed by 1500 LST (~3.5°C), at dawn (~3.2°C), and during the morning hours (~2°C), in that

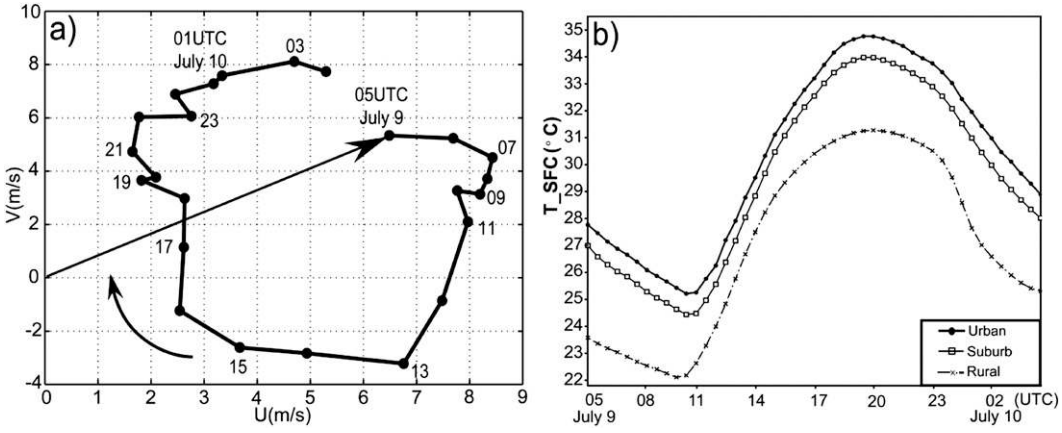

FIG. 7. (a) Hodograph of the horizontal winds in the urban PBL (i.e., layer-averaged between 500 and 1800 m) along the WBC, and (b) time series of the area-averaged T_{SFC} (°C) over the central business districts (solid dots) and low-intensity residential (squares) and rural (times signs) areas, both from the model simulation for the period of 0500 UTC 9 Jul–0500 UTC 10 Jul 2007.

order. On average, the urban–rural difference in T_{SFC} is about one-half of that in T_{SKIN}, and the surface air temperature over CBDs is about 1°C warmer than over suburban areas from noon to the following dawn. The nighttime UHI effects originate mostly from the release of sensible heat stored in concrete and asphalt during the daytime (Kusaka et al. 2001; Chen et al. 2004). It is clear that experiment NUCM could not reproduce such UHI effects because typical land surface schemes do not parameterize the associated processes. Despite the large urban–rural differences in T_{SFC} at any instant there is little difference in the amplitudes of diurnal variation of T_{SFC} between urban and rural regions.

4. Impact of upstream urbanization

After verifying the model performance in reproducing the UHI effects, we will use the model results to examine the impact of upstream urbanization on the generation of stronger UHI signals over Baltimore on 9 July. First, Figs. 8a and 8b show that the peak T_{SFC} and equivalent potential temperature θ_e over Baltimore's CBD depend on the horizontal wind direction and upstream land use, given the weak thermal gradients in the large-scale environment (Fig. 3). To be specific, the simulated T_{SFC} and θ_e at Baltimore are about 2° and 4°C higher on 9 July than on 8 July because of different wind directions. This is because the surface air in Baltimore originated from the upstream urban area (i.e., Columbia and even Washington) on 9 July when V_{SFC} is southwesterly (Fig. 8b), whereas it is from the upstream rural area on 8 July when V_{SFC} is near westerly (Fig. 8a). On the other hand, the simulated T_{SFC} and θ_e at both Baltimore and Washington are similar on 8 July, but they are at least 1° and 2°C warmer at Baltimore than at Washington on 9 July, respectively. In particular, an inverted-V-shaped pocket of warm air extends from Washington northeastward, showing the transport of the heated air along the WBC toward Baltimore in the presence of a southwesterly flow (Fig. 8b). In a similar way, the urban–rural T_{SFC} differences (i.e., UHI) are greater on 9 July (e.g., 6°C) than those on 8 July (e.g., 4°C).

The large T_{SFC} gradients (as high as 10°C over ~10 km) that appear along the coastline are the driving force for the development of the Chesapeake Bay breezes. The bay breezes behave differently on the two days, however, depending on the wind direction. The breezes are suppressed on 8 July, and instead a narrow zone of land breezes occurs offshore. By comparison, the bay breezes can penetrate as deep as 30 km over the rural area into Columbia on 9 July, with a pronounced θ_e gradient at the leading edge. The differences in θ_e are related more to temperature and moisture over urban and the bay regions, respectively. The bay breezes affect T_{SFC} near the harbor or shore region (see Figs. 8b and 6c) but have little effect in Baltimore's CBD. As a result, the westerly and southwesterly flows allow the urban warmer air along the WBC to extend more eastward, north and northeastward, respectively (cf. Figs. 8a,b). Such advective effects do not apply to T_{SKIN}, which is similar in magnitude and distribution during the two days, since it is a radiometric temperature due to the thermal emission of the earth's surface and is closely related to local properties of land cover/land use and soil texture.

Figure 9 shows the evolution of the along-flow PBL structures, in terms of θ' and in-plane flow vectors, that are taken through Washington, Columbia, and Baltimore during the early afternoon period (i.e., 1330–1630 LST) of

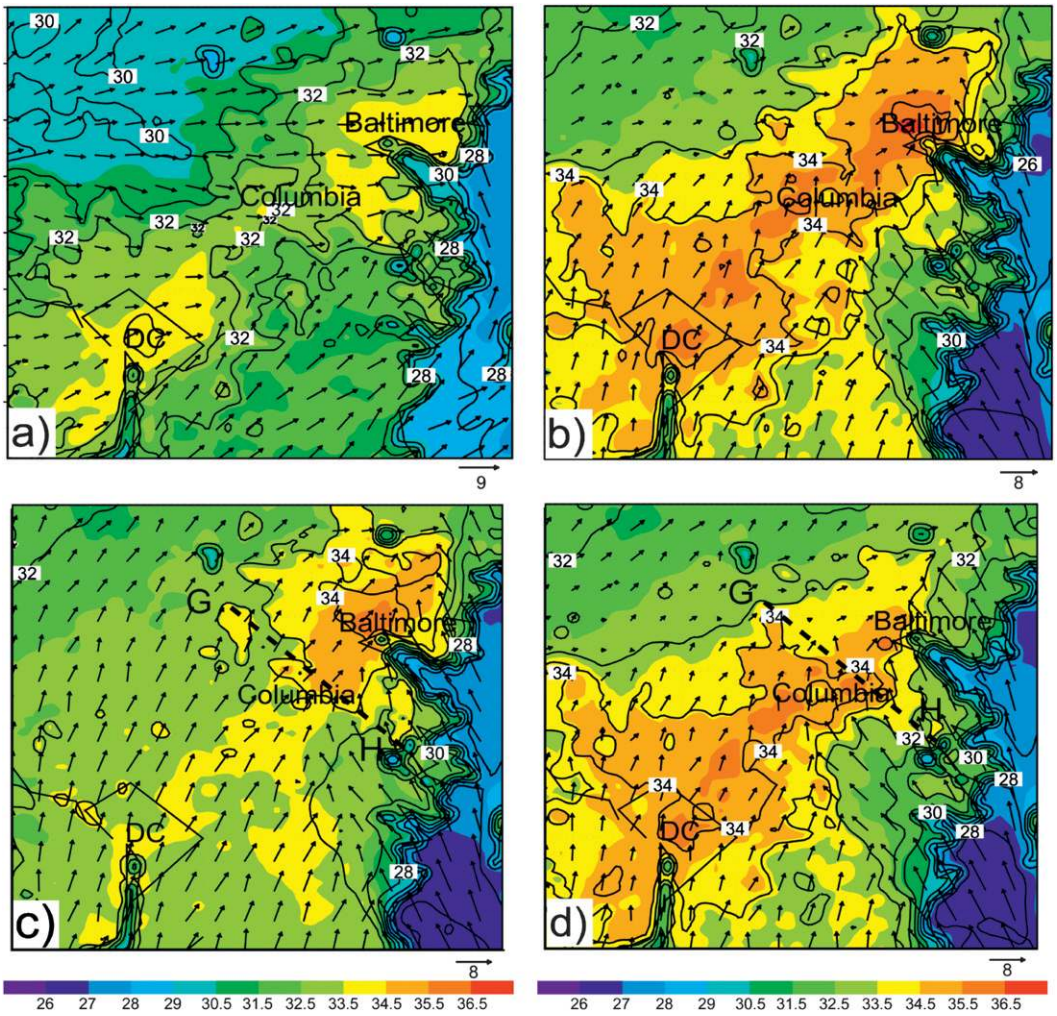

FIG. 8. Horizontal distribution of T_{SFC} (°C; shaded) and surface θ_e (solid contours; at 1°C intervals), superimposed with horizontal wind vectors plotted at 5-km grid intervals, from the (a) 32.5- and (b) 56.5-h simulations, valid at 2030 UTC 8 Jul and 9 Jul, respectively, over a subdomain of D4. As in (b), but for sensitivity simulations (c) NUH (treating the southwestern urban areas as rural area) and (d) RUR (treating Baltimore as a rural area). Thick dashed line G–H in (c) and (d) indicates the boundary of land-use changes used in expts NUH and RUR, respectively.

9 July, where the θ perturbation θ' is obtained by subtracting the area-averaged but time-dependent θ profile in the rural environment to the west of the WBC (see box R in Fig. 2a). Note that this along-flow cross section is taken by assuming that the larger-scale horizontal flows are at a near–steady state. Note also that Washington's CBD is not included in Fig. 9 because it is not directly at Baltimore's upstream. It is of particular importance that 1) the UHI warming effects extend upward as stratified hot plumes rooted at the urban surfaces and their intensities decrease upward, 2) the hot plumes correspond well to individual local towns along the WBC (cf. Figs. 9a and 2a), 3) these plumes are shallower near Washington and become deeper downstream toward Baltimore (see Figs. 9a–c), 4) more robust and wide hot plumes develop between Washington and Columbia likely because of the downstream transport of warm air from Washington's panhandle region (cf. Figs. 9 and 2), and 5) the plumes grow with time until reaching an altitude of $z = 1.4$ km in the late afternoon, which represents roughly the depth of the well-mixed PBL. To our knowledge, the previous studies have examined the UHI effects mostly in the context of T_{SFC} and T_{SKIN} but with little attention on such vertical UHI structures, likely because of the lack of high-resolution urban models.

Figure 9 also shows that deep rising motions on the scale of 2–20 km and as strong as 0.3 m s^{-1} occur in the wakes of individual major plumes in the well-mixed PBL, and up to 0.75 m s^{-1} in northern Baltimore where

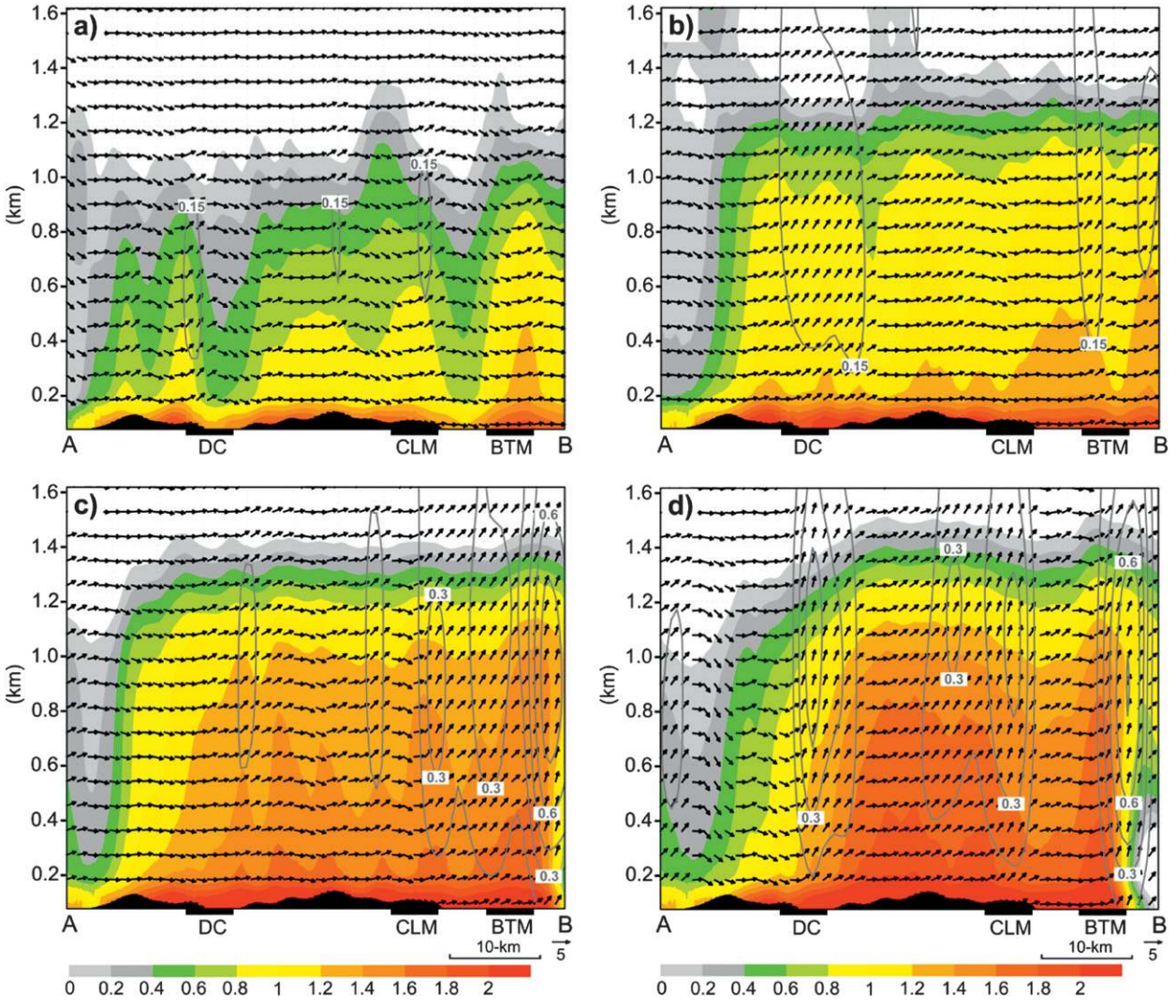

FIG. 9. Vertical cross sections of the potential temperature perturbations (shaded), and vertical motion (gray contours; m s^{-1}), superposed with in-plane flow vectors, along zone A–B (see Fig. 4d for the location) from (a) 53.5-, (b) 54.5-, (c) 55.5-, and (d) 56.5-h simulations, valid at 1730, 1830, 1930, and 2030 UTC 9 Jul 2007, respectively. Letters DC, CLM, and BTM denote the location of Washington, D.C., Columbia, and Baltimore, respectively.

the urban circulation and bay breezes meet (cf. Figs. 9d and 2a). Their peak magnitudes take place near $z = 1$–1.2 km (Figs. 9c,d) and become negative above $z = 4$ km at later stages (not shown). They are not likely part of gravity waves associated with the nearby topography (cf. Figs. 4a and 1) because the lapse rates are nearly neutral in the mixed layer and they are absent over the rural areas (e.g., Fig. 10a) and in the free troposphere (e.g., Figs. 9a–c). Upward motion of this magnitude could help to trigger cumulus clouds near the top of the PBL, the urban–rural boundaries, especially near the urban–bay breeze boundaries.

These clouds play a central role in atmospheric chemistry and air quality. Clouds and aerosols shield the lowest layers of the troposphere from UV radiation that drives photochemical smog (Dickerson et al. 1982; Shetter et al. 2003). Sulfuric acid (H_2SO_4) is produced rapidly by reaction between sulfur dioxide (SO_2) and hydrogen peroxide (H_2O_2) in cloud droplets; this pathway is the major source of sulfate, which is often the dominant component of aerosols. Cumulus clouds also vent the PBL, moving pollutants into the free troposphere where residence times are longer and impacts are larger (Loughner et al. 2011).

Of particular relevance to this study is that each layer of the surface-rooted hot plumes over Baltimore is generally deeper and more robust than those upstream, that is, over Columbia (Fig. 9), which is consistent with

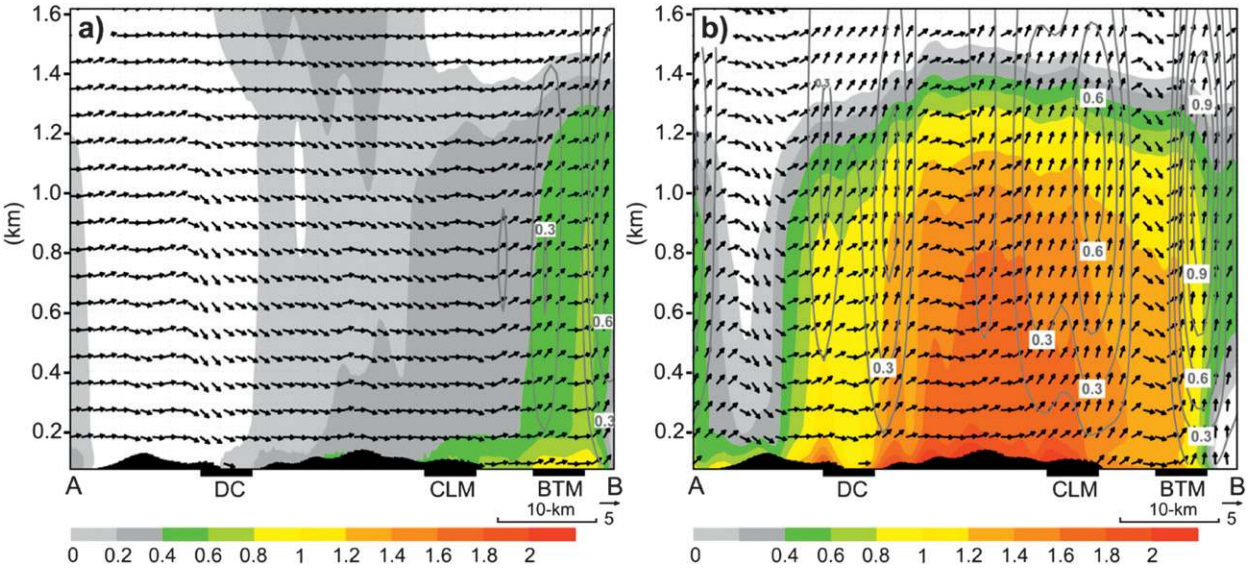

FIG. 10. As in Fig. 9d, but for the sensitivity simulations (a) NUH (treating the southwestern urban areas as rural area) and (b) RUR (treating Baltimore as a rural area).

the observational finding of Angevine et al. (2003) for the city of Nashville. As hypothesized earlier, this feature results from the upstream urbanization. To validate this hypothesis and to examine the impact of the southwesterly flows on Baltimore's UHI effects, two sensitivity experiments are conducted while holding all of the other parameters identical to the CTL run shown above. That is, in one run, the urban surfaces to the south of Baltimore are replaced by mixed forests (experiment NUH) that are similar to the land use over nearby rural areas (Fig. 2a), whereas in the other run, Baltimore is treated as a rural area (experiment RUR). The demarcation for the land-use changes is given as line G–H in Figs. 8c and 8d.

It is clear from Fig. 8c that, in the absence of upstream urbanization, surface heat sources to the southwest are gone and Baltimore is at least 1°C cooler in T_{SFC} (and θ_e) than in the control case. [The differenced T_{SFC} field between the CTL and NUH runs over a magnified Baltimore region, as given in Zhang et al. (2009), shows a citywide reduction in T_{SFC} in experiment NUH, with about 1.25°C peak differences or 25%-reduced UHI effects in the heart of Baltimore and at its southwestern corner.] As a result, experiment NUH produces a shallower (by ~200 m) mixed PBL with a much weaker hot plume over Baltimore than that in CTL (cf. Figs. 10a and 9d). A deeper PBL means that air pollutants are mixed into a greater volume over the city, and concentrations are reduced by dilution. The greater temperatures of the UHI lead to greater emissions and faster pollutant production and overwhelm the effects of dilution (EPA 2006). The UHI thus leads to more total pollution and pollutants lofted to higher altitudes; these factors may result in greater transport, with adverse effects on air quality and climate over larger areas.

The results clearly suggest the importance of horizontal advection of warm air generated over the upstream "heated islands" in CTL and of cold air over the upstream "rural areas" in NUH in determining the UHI effects in Baltimore. Note that the vertical motion to the south of Baltimore is mostly downward because of the influence of the Bermuda high, confirming further the importance of the urban-surface-rooted hot plumes in generating the pronounced upward motion. A slightly warmer PBL also occurs to the south of Baltimore, which can be attributed to the specification of mixed forests for urban surfaces as compared with nearby irrigated cropland surfaces (cf. Figs. 2a and 10a). It follows that Baltimore's UHI effects on 9 July would be much weaker in the absence of upstream urbanization.

The (nonlocal) advective impact of the UHI effects by southwesterly flows could be further seen by comparing between the CTL and RUR simulations (cf. Figs. 8b and 8d, and Figs. 9d and 10b). Results show little changes in T_{SFC} over the D.C. and Columbia areas, but Baltimore's T_{SFC} is higher than expected for a "rural" area (cf. Figs. 8b and 8d). In a similar way, a much weaker hot plume than that in CTL also appears over Baltimore (cf. Figs. 9d and 10b). The warm T_{SFC} and plume are obviously attributable to the advection of warmer air from Columbia and farther upstream.

While the above two sensitivity simulations, as compared with the CTL, reveal clearly the impact of thermal advection from the upstream urban area on the UHI

effects in Baltimore, one may wonder how the warmer T_{SFC} and hotter plume could be achieved since a similar amount of the warm air over Baltimore would be advected downstream. It is apparent that, because of the southwesterly advection of the warm air from the upstream heated PBL, little additional heat from the surface would be needed to maintain the warm column above Baltimore. Instead, most of the local surface heat fluxes will be used to heat the column and increase the depth of the mixed PBL. Then, entrainment into the potentially warmer air aloft helps to further increase the potential temperature in the mixed PBL (Zhang and Anthes 1982), thereby leading to the generation of the more-robust hot plumes over the city of Baltimore.

One may note from Figs. 8, 9d, and 10 that urbanization along the WBC alters not only the lower tropospheric temperature but also the wind field. Without the urban development in Washington and Columbia, the daytime surface winds would be stronger, even over Baltimore, because of the presence of less surface friction (cf. Figs. 8b and 8c). The bay breezes could penetrate farther inland when Baltimore is treated as rural (cf. Figs. 8b and 8d), and stronger convergence and upward motion occur on the downstream side of Baltimore (cf. Figs. 9d and 10b). Weaker winds allow the buildup of greater pollution concentrations.

5. Structures and evolution of the urban and rural boundary layers

After seeing the along-flow structures of hot plumes (or the mixed layer) over the WBC, it is desirable to examine their normal-flow circulations and the differences in PBL structures between urban and rural regions. By comparing Figs. 11a and 9d we see very different PBL structures along the WBC on 8 July when compared with those occurring on 9 July because of different wind directions. For instance, more significant hot plumes take place over the region between Washington and Columbia because of the downstream (near westerly) transport of heated air from Washington's panhandle region (Fig. 11a). Baltimore exhibits little difference from that in the upstream rural area. In particular, the overall UHI effects in the PBL are relatively small, like the corresponding surface map (cf. Figs. 11c and 8a), but they are in marked contrast to the T_{SKIN} map (cf. Figs. 11c and 4b). Thus, it is more appropriate to use T_{SFC} *rather than* T_{SKIN} *as a proxy for UHI effects* when the nonlocal processes are pronounced (Jin et al. 2005).

Despite the presence of less-robust plumes, the mixed-layer depth on 8 July could still reach as high as 1.4 km, similar to heights seen on 9 July (cf. Figs. 9 and 11c). It is apparent that the intensity of hot plumes, denoted by the urban–rural θ' magnitude, is determined by upstream PBL warmth and local surface heating, given the identical distribution and magnitude of T_{SKIN} as the bottom boundary conditions. Because of the less-robust plumes, fewer and weaker upward-motion bands occur along the WBC on 8 July. This suggests that the initiation of thunderstorms through the UHI effects, as studied by Ntelekos et al. (2007), tends to be less frequent when the WBC is dominated by westerly flows than when under the influence of southwesterly flows.

Figures 11b and 11c compare the vertical cross-sectional structures of the PBL through Baltimore and its vicinity, especially normal to the bay-breeze front, on 8 and 9 July. For 9 July, one can see clearly more robust hot plumes with a deeper mixed layer over the city, a deeper layer of the bay breezes (up to 0.8 km in Fig. 11c), and sharper upward motion at the leading bay-breeze front, with evident compensating subsidence on both sides. Associated with the sharp upward motion are one branch of weak compensating subsidence to the west that delineates roughly the interface between the urban and rural boundary layers and another branch to the east that produces weak warming above the bay boundary layer (Fig. 11c).

It is also evident from Fig. 11b that more-robust plumes with significant UHI effects tend to occur on the downwind side, consistent with the hypothesis validated above; a weak, suspended "urban plume" caused by thermal advection, is more extensive to the northeast of Baltimore on 9 July (see Shou and Zhang 2010) and overlies a shallow bay boundary layer. Like the UHI-induced circulations, convective initiation would likely occur more frequently along the bay-breeze front under the influence of south to southwesterly flows, as compared with that influenced by westerly flows (Figs. 11b,c). Shou and Zhang (2010) showed that urban plumes could be advected far downstream even after sunset, making suburban areas warmer than in the city. Such nonlocal UHI effects appear to have important implications to the understanding of many air quality and environmental problems.

Figure 12 compares the vertical profiles of the area-averaged θ at 2-hourly intervals during the daytime over a representative urban area (U; i.e., at Baltimore's CBD) and a rural area (R) along the WBC (see Fig. 2a for their locations). Although the two sample points are only about 40 km apart, the urban–rural differences are evident. There is always a superadiabatic layer in the lowest 100–200 m a couple of hours before sunset over the rural region. By 1900 LST a strong inversion layer has developed as a result of intense outgoing radiation. In contrast, the superadiabatic lapse rate over the urban region is much stronger than that over the rural region; it

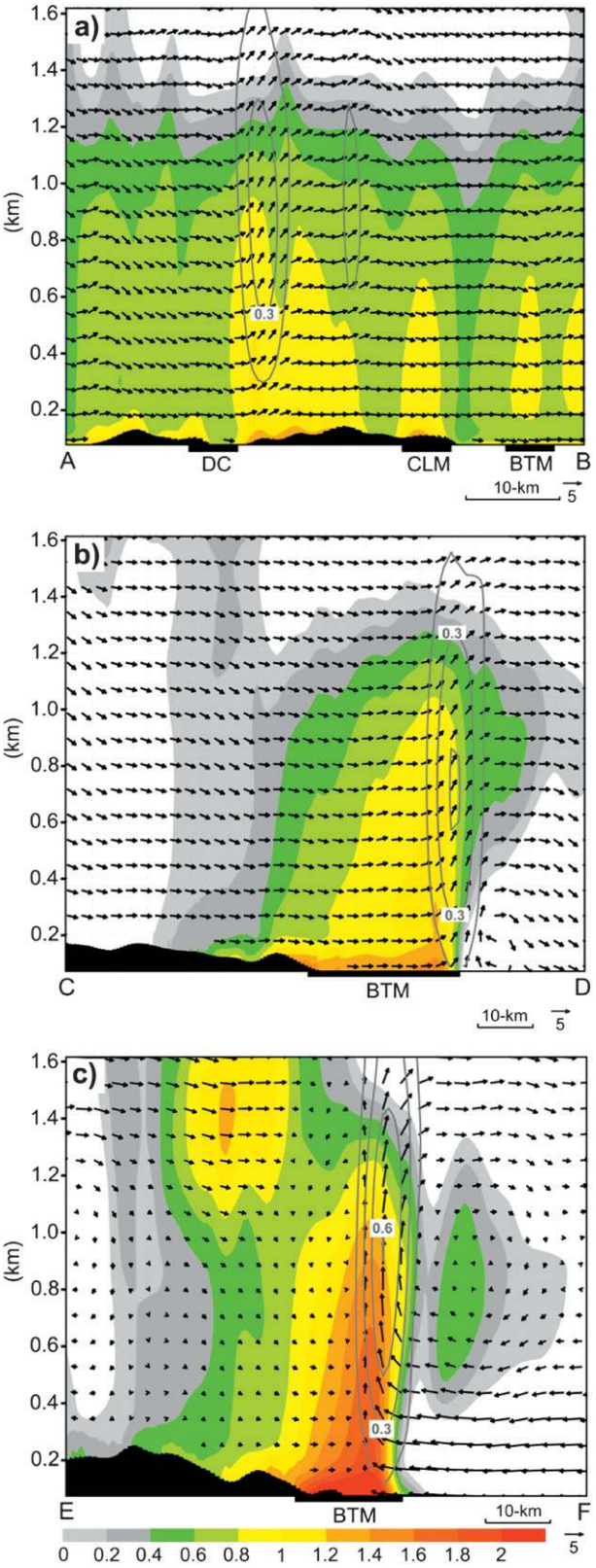

FIG. 11. Vertical cross sections of the potential temperature perturbations (shaded) and vertical motion (gray solid contours; m s^{-1}), superposed with in-plane flow vectors, from the 32.5-h simulation, valid at 2030 UTC 8 Jul (a) normal to the mean flow along zone A–B given in Fig. 4d, (b) along the mean flow along zone C–D given in Fig. 4b, and (c) as in (a) but from 56.5-h simulation, valid at 2030 UTC 9 Jul along zone E–F given in Fig. 4d.

could still occur at 1900 LST, and even a few hours after sunset (not shown), because of the release of sensible heat stored in impervious surfaces (e.g., from high-rises).

In addition, the urban mixed layer is heated at greater rates than is the rural mixed layer, especially during the early morning hours (e.g., at 0700 LST) when they are shallow; the former also grows in depth faster than the latter. Moreover, the urban–rural θ' becomes smaller with time as the mixed layers deepen; in its middle portion the θ' value decreases from 1.5°C at 0700 LST to 0.2°C at 1500 LST. The variation of the urban–rural θ' is opposite to that of the urban–rural T_{SFC} differences (cf. Figs. 7b and 12). Namely, the latter is weakest during the early morning hours and peaked near 1500 LST as a result of the different rates in storing sensible heat, as discussed in section 1.

The urban mixed layer exhibits marked cooling near sunset, for example, as large as 3°C near $z = 100$ m at 1900 LST, whereas on average the urban T_{SFC} shows little change (cf. Figs. 7b and 12). This cooling is clearly an important evidence of the bay-breeze intrusion into the city of Baltimore, as mentioned before (see Figs. 6 and 8b). The bay breezes are as deep as 600–800 m (Fig. 11b) and last for several evening hours. The urban T_{SFC} and T_{SKIN}, however, would experience much less influence of the bay breezes, except near its harbor region, because of the effects of surface friction. As a result, the bay breezes generate an intense inversion layer (e.g., 1.5°C between 100 and 400 m) at 1900 LST in the lower portion of the urban mixed layer, and a superadiabatic layer below that is much stronger than that during the daytime. This result indicates the important influence of DLC-induced circulations on the UHI effects and urban PBL structures, and such influence may differ from city to city and time to time, depending the magnitude and direction of mean flows.

6. Summary and conclusions

In this study, we examined an extreme UHI event that occurred over Baltimore on 9 July 2007 and tested the hypothesis that the UHI event can be markedly enhanced by upstream urbanization. This is achieved by performing ultrahigh-resolution control and sensitivity

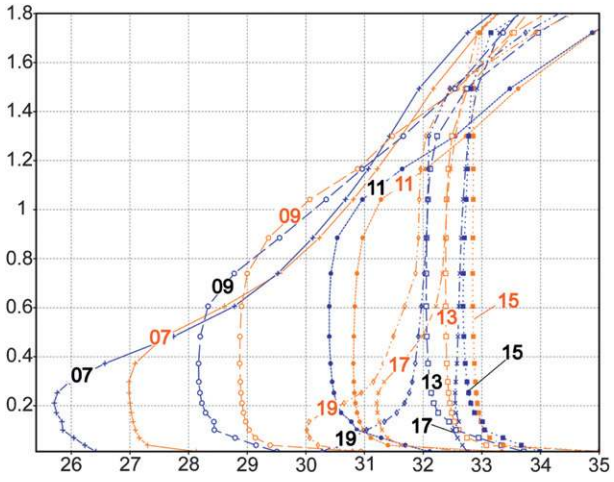

FIG. 12. Vertical profiles of the area-averaged potential temperature (°C), at 2-hourly intervals, over an urban (U; colored in orange) and rural (R; colored in blue) area during the period of 0700–1900 LST 9 Jul 2007. See Fig. 2a for the locations of boxes U and R.

simulations using a coupled model consisting of WRF–Noah–UCM with the NLCD 2001 land-use data. Results show that the coupled model could reproduce the observed UHI event in terms of T_{SKIN} and T_{SFC}, such as the 5°C (10°C) T_{SFC} (T_{SKIN}) contrasts between the urban and rural areas, the diurnal variations of T_{SFC} and horizontal winds around the WBC, as well as the bay breezes. In particular, the vertical growth and structures of the UHI effects are shown as layered hot plumes rooted at the urban surfaces with pronounced rising motions.

A comparison between the control and two sensitivity simulations reveals the important roles of upstream urbanization in enhancing the UHI effects over Baltimore through (nonlocal) advective processes. Without the upstream urbanization, the UHI effects over Baltimore would be 1.25°C weaker, or reduced by 25%, with a 200-m-shallower mixed PBL and a much less robust hot plume (Zhang et al. 2009); this may cause a significant reduction in surface pollution ozone concentration and even greater reduction in column content. The enhanced UHI effects are argued to result from the (nonlocal) thermal advection of warm air upstream, the local upward surface heat fluxes, and entrainment of the potentially warmer air aloft. These results indicate the importance of considering the possible enhanced UHI effects as a result of inadvertent upstream urbanization. The nonlocal effects also indicate that T_{SFC} rather than T_{SKIN} should be used to study UHI effects when V_{SFC} is pronounced because of the advective effects for T_{SFC}.

Results also show different PBL structures between urban and rural regions, especially when interacting with the bay-breeze circulations. The urban mixed layer tends to grow faster and deeper, and have a larger superadiabatic lapse rate in its bottom 100-m layer, than those of the rural mixed layer. A superadiabatic bottom layer could exist even a few hours after sunset because of the release of sensible heat stored in buildings during the daytime. It is found that the interaction of the UHI effects with the bay breezes depends on wind direction. Under favorable conditions, the cold intrusion of the bay breezes may generate a strong inversion above and an ultra-superadiabatic layer below. The urban T_{SFC} and T_{SKIN} would experience much less influence of the bay breezes, however, because of the surface frictional effects. The results suggest that the coupled model could be useful for improving the prediction of near-surface flows, the initiation of moist convection, air quality, visibility, and other environment-related variables.

Acknowledgments. This work was funded by Maryland's Department of Environment. Surface observations plotted in Fig. 6 were obtained from NOAA/National Severe Storms Laboratory Historical Weather Data Archives from their Web site at http://data.nssl.noaa.gov.

REFERENCES

Allwine, K. J., J. H. Shinn, and G. E. Streit, 2002: Overview of URBAN 2000: A multiscale field study of dispersion through an urban environment. *Bull. Amer. Meteor. Soc.,* **83,** 521–536.

Angevine, W. M., A. B. White, C. J. Senff, M. Trainer, R. M. Banta, and M. A. Ayoub, 2003: Urban–rural contrasts in mixing height and cloudiness over Nashville in 1999. *J. Geophys. Res.,* **108,** 4092, doi:10.1029/2001JD001061.

Arnfield, A. J., 2003: Two decades of urban climate research: A review of turbulence, exchanges of energy and water, and the urban heat island. *Int. J. Climatol.,* **23,** 1–26.

Atkinson, B. W., 2003: Numerical modeling of urban heat island intensity. *Bound.-Layer Meteor.,* **109,** 285–310.

Banta, R. M., and Coauthors, 1998: Daytime buildup and nighttime transport of urban ozone in the boundary layer during a stagnation episode. *J. Geophys. Res.,* **103,** 22 519–22 544.

Bernstein, L., and Coauthors, Eds., 2007: *Climate Change 2007: Synthesis Report*. Cambridge University Press, 104 pp.

Bloomer, B. J., J. W. Stehr, C. A. Piety, R. J. Salawitch, and R. R. Dickerson, 2009: Observed relationships of ozone air pollution with temperature and emissions. *Geophys. Res. Lett.,* **36,** L09803, doi:10.1029/2009GL037308.

——, R. R. Dickerson, and K. Vinnikov, 2010: A chemical climatology and trend analysis of ozone and temperature over the eastern US. *Atmos. Environ.,* **44,** 2543–2551.

Bornstein, R. D., 1968: Observations of the urban heat island effect in New York City. *J. Appl. Meteor.,* **7,** 575–582.

——, and Q. L. Lin, 2000: Urban heat islands and summertime convective thunderstorms in Atlanta: Three case studies. *Atmos. Environ.,* **34,** 507–516.

Brazel, A., N. Selover, R. Vose, and G. Heisler, 2000: The tale of two climates—Baltimore and Phoenix urban LTER sites. *Climate Res.,* **15,** 123–135.

Chen, F., and J. Dudhia, 2001: Coupling an advanced land surface–hydrology model with the Penn State–NCAR MM5 modeling system. Part I: Model implementation and sensitivity. *Mon. Wea. Rev.,* **129,** 569–585.

——, H. Kusaka, M. Tewari, J. W. Bao, and H. Hirakuchi, 2004: Utilizing the coupled WRF/LSM/urban modeling system with detailed urban classification to simulate the urban heat island phenomena over the greater Houston area. Preprints, *Fifth Conf. on Urban Environment,* Vancouver, BC, Canada, Amer. Meteor. Soc., 9.11. [Available online at http://ams.confex.com/pdfpapers/79765.pdf.]

——, and Coauthors, 2010: The integrated WRF/urban modeling system: Development, evaluation, and applications to urban environmental problems. *Int. J. Climatol.,* **31,** 273–288.

Cheng, Y. Y., and D. W. Byun, 2008: Application of high resolution land use and land cover data for atmospheric modeling in the Houston–Galveston metropolitan area, Part I: Meteorological simulation results. *Atmos. Environ.,* **42,** 7795–7811.

Chou, M.-D., and M. J. Suarez, 1994: An efficient thermal infrared radiation parameterization for use in general circulation models. NASA Tech. Memo. 104606, 85 pp.

Dickerson, R. R., D. H. Stedman, and A. C. Delany, 1982: Direct measurements of ozone and nitrogen-dioxide photolysis rates in the troposphere. *J. Geophys. Res.,* **87,** 4933–4946.

EPA, 2006: Air quality criteria for ozone and related photochemical oxidants. EPA Rep. EPA/600/R-05/0004aA. [Available online at http://cfpub.epa.gov/ncea/cfm/recordisplay.cfm?deid=149923.]

Grell, G. A., and D. Devenyi, 2002: A generalized approach to parameterizing convection combining ensemble and data assimilation techniques. *Geophys. Res. Lett.,* **29,** doi:10.1029/2002GL015311.

Grossman-Clarke, S., J. A. Zehnder, W. L. Stefanov, Y. Liu, and M. A. Zoldak, 2005: Urban modifications in a mesoscale meteorological model and the effects on near-surface variables in an arid metropolitan region. *J. Appl. Meteor.,* **44,** 1281–1297.

Holt, T., and J. Pullen, 2007: Urban canopy modeling of the New York City metropolitan area: A comparison and validation of single- and multilayer parameterizations. *Mon. Wea. Rev.,* **135,** 1906–1930.

Hong, S. Y., J. Dudhia, and S. H. Chen, 2004: A revised approach to ice microphysical processes for the bulk parameterization of clouds and precipitation. *Mon. Wea. Rev.,* **132,** 103–120.

Imhoff, M. L., P. Zhang, R. E. Wolfe, and L. Bounoua, 2010: Remote sensing of the urban heat island effect across biomes in the continental USA. *Remote Sens. Environ.,* **114,** 504–513.

Jacob, D. J., and D. A. Winner, 2009: Effect of climate change on air quality. *Atmos. Environ.,* **43,** 51–63.

Janjić, Z. I., 1994: The step-mountain eta coordinate model: Further development of the convection, viscous sublayer, and turbulent closure schemes. *Mon. Wea. Rev.,* **122,** 927–945.

Jin, M., R. E. Dickinson, and D.-L. Zhang, 2005: The footprint of urban areas on global climate as characterized by MODIS. *J. Climate,* **18,** 1551–1565.

Kalnay, E., and M. Cai, 2003: Impact of urbanization and land-use change on climate. *Nature,* **423,** 528–531.

Kunkel, K. E., S. A. Changnon, B. C. Reinke, and R. W. Arritt, 1996: The July 1995 heat wave in the Midwest: A climatic perspective and critical weather factors. *Bull. Amer. Meteor. Soc.,* **77,** 1507–1518.

Kusaka, H., H. Kondo, Y. Kikegawa, and F. Kimura, 2001: A simple single-layer urban canopy model for atmospheric models: Comparison with multi-layer and slab models. *Bound.-Layer Meteor.,* **101,** 329–358.

Landsberg, H. E., 1979: Atmospheric changes in a growing community (the Columbia, Maryland experience). *Urban Ecol.,* **4,** 53–81.

——, 1981: *The Urban Climate*. International Geophysical Series, Vol. 28, Academic Press, 288 pp.

Loughner, C. P., D. J. Allen, K. E. Pickering, R. R. Dickerson, D.-L. Zhang, and Y. X. Shou, 2011: Impact of fair-weather cumulus clouds and the Chesapeake Bay breeze on pollutant transport and transformation. *Atmos. Environ.,* **45,** 4060–4072.

Martilli, A., A. Clappier, and M. W. Rotach, 2002: An urban surface exchange parameterization for mesoscale models. *Bound.-Layer Meteor.,* **104,** 261–304.

Mellor, G. L., and T. Yamada, 1974: Hierarchy of turbulence closure models for planetary boundary layers. *J. Atmos. Sci.,* **31,** 1791–1806.

Miao, S., and F. Chen, 2008: Formation of horizontal convective rolls in urban areas. *Atmos. Res.,* **89,** 298–304.

——, ——, M. A. LeMone, M. Tewari, Q. Li, and Y. Wang, 2009: An observational and modeling study of characteristics of urban heat island and boundary layer structures in Beijing. *J. Appl. Meteor. Climatol.,* **48,** 484–501.

Mlawer, E. J., S. J. Taubman, P. D. Brown, M. J. Iacono, and S. A. Clough, 1997: Radiative transfer for inhomogeneous atmosphere: RRTM, a validated correlated-*k* model for the longwave. *J. Geophys. Res.,* **102,** 16 663–16 682.

Ntelekos, A. A., J. A. Smith, and W. F. Krajewski, 2007: Climatological analyses of thunderstorms and flash floods in the Baltimore metropolitan region. *J. Hydrol.,* **8,** 88–101.

Ohashi, Y., and H. Kida, 2004: Local circulations developed in the vicinity of both coastal and inland urban areas. Part II: Effects of urban and mountain areas on moisture transport. *J. Appl. Meteor.,* **43,** 119–133.

Oke, T. R., 1973: City size and the urban heat island. *Atmos. Environ.,* **7,** 769–779.

——, 1987: *Boundary Layer Climates*. 2nd ed. Routledge, 464 pp.

——, 1995: The heat island characteristics of the urban boundary layer: Characteristics, causes and effects. *Wind Climate in Cities,* Kluwer Academic, 81–107.

Rotach, M. W. L., and Coauthors, 2005: BUBBLE—An urban boundary layer meteorology project. *Theor. Appl. Climatol.,* **81,** 231–261.

Rozoff, C. M., W. R. Cotton, and J. O. Adegoke, 2003: Simulation of St. Louis, Missouri, land use impacts on thunderstorms. *J. Appl. Meteor.,* **42,** 716–738.

Shetter, R. E., and Coauthors, 2003: Photolysis frequency of NO_2: Measurement and modeling during the International Photolysis Frequency Measurement and Modeling Intercomparison (IPMMI). *J. Geophys. Res.,* **108,** 8544, doi:10.1029/2002JD002932.

Shou, Y., and D.-L. Zhang, 2010: Impact of environmental flows on the urban daytime boundary layer structures over the Baltimore metropolitan region. *Atmos. Sci. Lett.,* **11,** 1–6. [Available online at doi:10.1002/asl.252.]

Skamarock, W. C., J. B. Klemp, J. Dudhia, D. O. Gill, D. M. Barker, W. Wang, and J. G. Powers, 2005: A description of the Advanced Research WRF version 2. NCAR Tech. Note NCAR/TN–468+STR, 100 pp.

Tai, A. P. K., L. J. Mickley, and D. J. Jacob, 2010: Correlations between fine particulate matter (PM2.5) and meteorological variables in the United States: Implications for the sensitivity of PM2.5 to climate change. *Atmos. Environ.,* **44,** 3976–3984.

Viterito, A., 1989: Changing thermal topography of the Baltimore-Washington corridor: 1950–1979. *Climatic Change,* **14,** 89–102.

Vukovich, F. M., and J. Sherwell, 2003: An examination of the relationship between certain meteorological parameters and surface ozone variations in the Baltimore–Washington corridor. *Atmos. Environ.,* **37,** 971–981.

Wan, Z., 2008: New refinements and validation of the MODIS land-surface temperature/emissivity products. *Remote Sens. Environ.,* **112,** 59–74.

——, and Z. L. Li, 2008: Radiance-based validation of the V5 MODIS land-surface temperature product. *Int. J. Remote Sens.,* **29,** 5373–5395.

Weaver, C. P., and Coauthors, 2009: A preliminary synthesis of modeled climate change impacts on U.S. regional ozone concentrations. *Bull. Amer. Meteor. Soc.,* **90,** 1843–1863.

Zhang, D., and R. A. Anthes, 1982: A high-resolution model of the planetary boundary-layer—Sensitivity tests and comparisons with SESAME-79 data. *J. Appl. Meteor.,* **21,** 1594–1609.

——, and W. Zheng, 2004: Diurnal cycles of surface winds and temperatures as simulated by five boundary layer parameterizations. *J. Appl. Meteor.,* **43,** 157–169.

——, S. Zhang, and S. Weaver, 2006: Low-level jets over the Mid-Atlantic states: Warm-season climatology and a case study. *J. Appl. Meteor. Climatol.,* **45,** 194–209.

——, Y. Shou, and R. Dickerson, 2009: Upstream urbanization exacerbates urban heat island effects. *Geophys. Res. Lett.,* **36,** L24401, doi:10.1029/2009GL041082.